Detecting the severity of woodwasp, *Sirex noctilio*, infestation in a pine plantation in KwaZulu-Natal, South Africa, using texture measures calculated from high spatial resolution imagery

M. Dye, O. Mutanga* & R. Ismail

Department of Geography, University of KwaZulu-Natal, Private Bag X01, Scottsville, 3209 South Africa

This study was undertaken to determine whether image texture derived from high spatial resolution imagery could successfully predict *Sirex noctilio* infestation levels in a pine plantation forest in the eastern part of South Africa. The woodwasp, *S. noctilio,* damages trees by releasing toxic mucus into the wood during oviposition. A 50 × 50 m grid was generated over the study area and 65 cells were randomly selected. Within each cell, a 10 m circular plot was created and the level (%) of *S. noctilio* infestation was visually assessed. Using high spatial resolution imagery (0.5 m), 13 texture measures were calculated with various window sizes. Correlation tests were then performed to determine the relationship between image texture and *S. noctilio* infestation levels. Individual correlations were average in strength. Consequently, a stepwise multiple linear regression analysis was undertaken to determine whether a selection of texture images could result in a more accurate prediction of *S. noctilio* infestation levels. A strong correlation of $r = 0.7$ between the predicted and the observed levels of *S. noctilio* infestation using the developed multiple linear regression model showed that image texture is a promising tool for the detection, and ultimately mapping, of *S. noctilio* infestation in plantations. The result is critical for improving the management of insect infestation in plantations of South Africa.

Key words: forest health, *Sirex noctilio,* high resolution images, texture analysis.

INTRODUCTION

The woodwasp, *Sirex noctilio,* which originated in Eurasia and North Africa (USDA 2000), is causing considerable damage in the pine plantation forests of KwaZulu-Natal in South Africa (Fig. 2). Detecting and mapping the severity of damage caused by this wasp on plantation forests is an important component of an integrated management strategy that aims at reducing their devastating impact. *Sirex noctilio* was first discovered in South Africa on the Cape Peninsula in 1994. Within eight years of its discovery, it had spread 380 km along both western and eastern coasts (Tribe & Cillie 2004). By 2002, *S. noctilio* had spread into the province of KwaZulu-Natal where it is currently causing considerable damage (Tribe 2006). The female wasp drills into the tree to deposit her eggs, normally 1–3 at a time (Hoebeke *et al.* 2005). During oviposition, the female introduces toxic mucus and the symbiotic fungus, *Amylostereum areolatum,* into the wood. When the tree's defences are overcome, the eggs hatch and the larvae feed on the fungus while tunnelling through the wood towards the centre of the tree. The wood becomes riddled with tunnels and fungus, causing the foliage to wilt, and weaker trees may die (Zondag & Nuttall 1999). Upon reaching the heartwood, the larvae make a U-turn and pupate below the bark (Tribe 2006). The longest part of this life cycle is spent inside the host tree (Slippers *et al.* 2003) and the larvae eventually emerge as adults by chewing round exit holes (Carlson & Verschoor 2006). Older trees are more at risk, but if the population of *S. noctilio* is not controlled, young and healthy trees can also be affected (Forestry Tasmania 1999).

The primary control for *S. noctilio* is achieved through biological agents (Tribe & Cillie 2004). Other methods include sanitation and salvage, where infected trees are removed; and thinning where weaker trees, which are more susceptible to *S. noctilio* infestation, are felled (USDA 2000).

Successful implementation of these control methods depend on the availability of spatially explicit maps that quantify the severity and extent of infestation (Ismail *et al.* 2006). Remote sensing combined with groundtruth data can offer useful techniques for the measurement of forest health decline (Yuan *et al.* 1991; Ismail *et al.* 2006). Methods using remotely sensed imagery can cover very

*Author to whom correspondence should be addressed.
E-mail: mutangao@ukzn.ac.za

Class	Stage	Crown condition	Picture	Symptom
1	Previsual	Healthy		No sign of *S. noctilio* infestation
2	Previsual	Green		Tree has been infected and resin droplets can be seen. No change in tree crown
3	Visual	Red		Tree starts to wilt and canopy colour changes to a reddish brown
4	Visual	Grey		100 % needle loss. Emergence holes visible on trunk

Fig. 1. Stages of *Sirex noctilio* infestation (adapted from Ismail *et al.* 2006).

large areas and provide timely and accurate information on a continual basis (Yuan *et al.* 1991; Katsch & Vogt 1999). One approach to predicting forest health using remote sensing has been the use of spectral information such as vegetation indices (Ismail *et al.* 2006; Franklin *et al.* 2003; Haara *et al.* 2002). Trees under stress show a decreased canopy reflectance in the lower portion of the infrared, reduced absorption in the chlorophyll active band, and a shift in the red edge (Carter & Knapp 2001). There is spatial dependence or correlation contained in vegetation and its radiation (Atkinson *et al.* 1992; Mutanga & Rugege 2006). As a result, research has been undertaken on how to improve spectral analysis and develop alternatives that integrate spatial information (King 2000).

Texture analysis is one useful technique in this regard. It is a spatially based image transformation technique which enhances the relationship between neighbouring pixels in an image for accurately predicting forest health. A number of studies have used image texture analysis to quantify forest damage as a result of pest infestation. Texture analysis was used to detect sugar maple leaf decline in northeastern America. The study concluded that variations in the tree crowns as a result of health decline could be quantified through a linear model, which related the changes to the image texture (Yuan *et al.* 1991). Moskal & Franklin (2004) showed a strong relationship between image

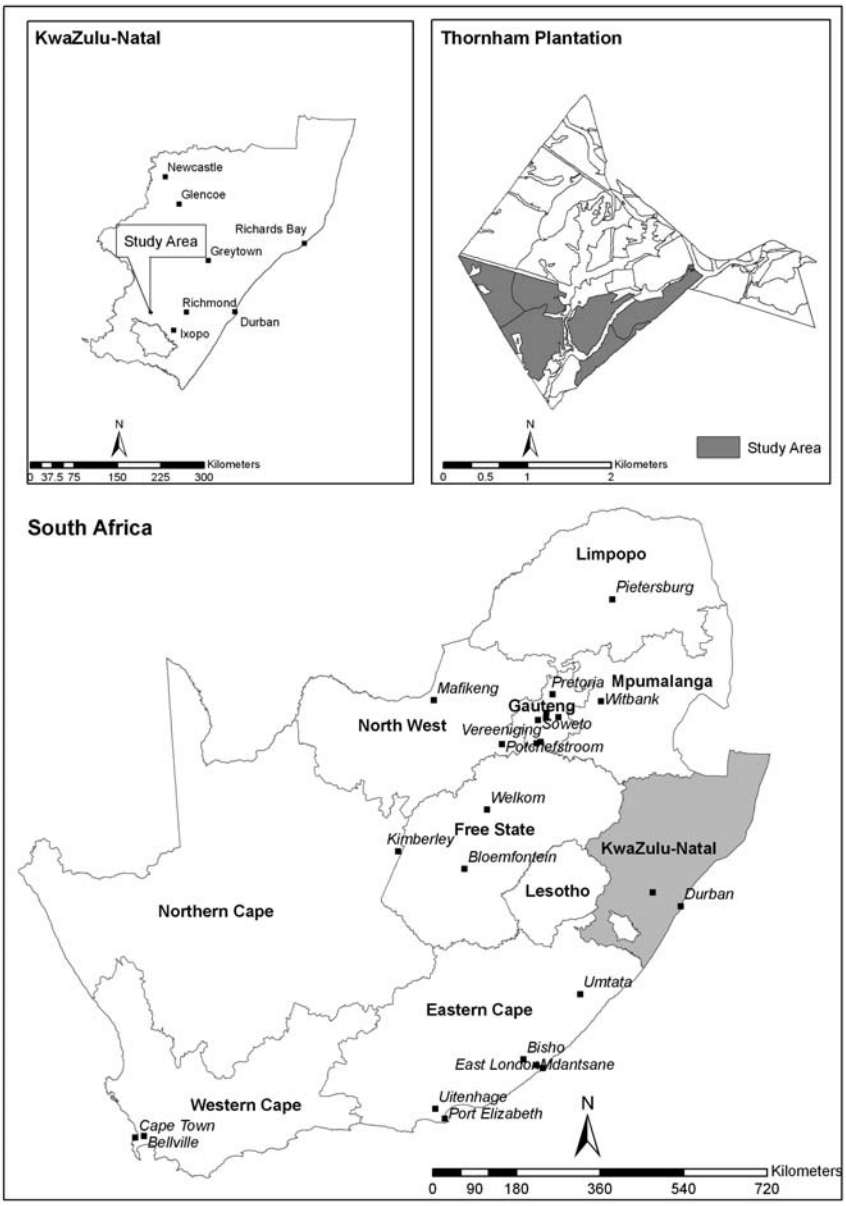

Fig. 2. Location of the study area.

texture measures from CASI bands and defoliation severity of aspen, *Populus tremuloides* Michx. The application of this technique to quantify the visual stages of *S. noctilio* infestation (see Fig. 1) has, to our knowledge, not been previously undertaken. The aim of this study was to determine whether texture images calculated from high spatial resolution imagery (0.5 m) could accurately predict the levels of damage caused by *S. noctilio* infestation.

MATERIAL AND METHODS

Location of study area

The study area is part of the Mondi Thornham plantation (Fig. 3) and is situated in the Midlands area of KwaZulu-Natal, South Africa. The size of the study area is 356 ha and it lies at an altitude of 1500 m a.s.l. Rainfall varies between 800 mm and 1200 mm per year (Schulze *et al.* 1997).

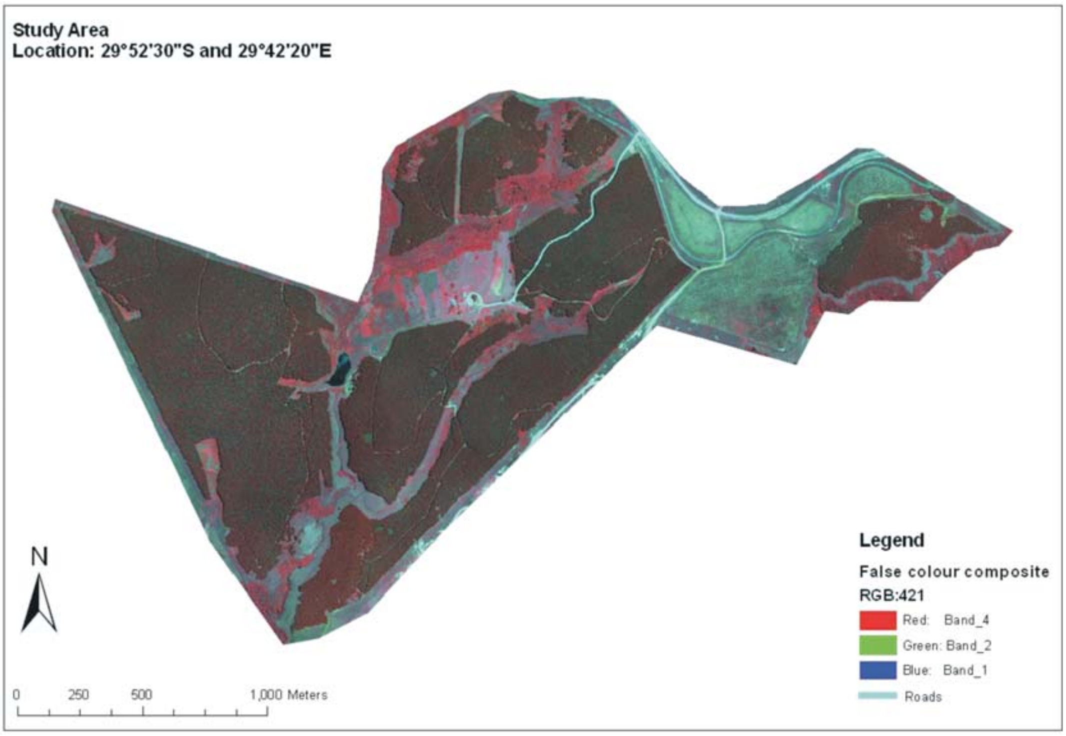

Fig. 3. Mondi Thornham Plantation.

Data acquisition

Very high resolution imagery (0.5 m) was obtained on 24 November 2005 by Land Resources International (LRI) using their LREye aerial image system which is composed of a series of four monochrome Sony cameras (Table 1; Ismail *et al.* 2006). Imagery was supplied as colour (RGB) and false colour infrared (NIR) tiles.

Field data collection

Field data collection took place within the period of image acquisition from 10 November to 30 November 2005. A 50 × 50 m grid was generated over the study area and 65 cells were randomly selected. At the centre point of each grid cell, a 10 m circular plot was created. Tree crowns located within each plot were manually identified on the high resolution imagery and subsequently located in the field using a Global Positioning System (GPS). The trees were assessed for *S. noctilio* infestation levels with the help of experienced foresters and technical staff. To prevent errors of commission, trees identified as red stage trees, those having a reddish brown canopy, were destructively sampled to check for the presence of *S. noctilio* larvae. Results from destructive sampling showed that all trees that had been identified as infested actually contained *S. noctilio* larvae. The level of *S. noctilio* infestations was calculated by measuring the percentage of infested trees from the total number of trees in the plot.

Texture analysis

Images consist of tone (spectral variation) and texture (spatial variability). Image texture is significant as it gives important information about the spatial arrangement of objects in an image (Myint & Lam 2005). Texture statistics can be divided into two classes: first-order (occurrence)

Table 1. Spectral bands from high resolution imagery used in the study.

Band	Colour	Spectral range (nm)	Spatial resolution (m)
1	Blue (B)	450–480	0.5
2	Green (G)	550–580	0.5
3	Red (R)	650–680	0.5
4	Near infrared (NIR)	850–900	0.5

and second-order (co-occurrence). First-order statistics are obtained from the histogram of pixel intensities within a neighbourhood or window, but do not take into account the spatial relationship between pixels. Second-order statistics on the other hand calculate the probability that each pair of pixel values within a moving window co-occur in a given direction of distance (St-Louis *et al.* 2006). Second-order texture measures are calculated from the grey level co-occurrence matrix (GLCM) proposed by Haralick *et al.* (1973) and have become the most well-known and widely used texture features (Kayitakire *et al.* 2006). The co-occurrence method finds the conditional joint probabilities of all pairwise combinations of grey levels within a spatial window. The set of grey level co-occurring probabilities (GLCP) are stored in the GLCM, and statistics are applied to the matrix in order to generate texture features which are assigned to the centre pixel of the moving window (Jobanputra 2006). First-order texture measures are fast and easy to implement, while second-order measures are seen as being a better texture representation method (Yuan *et al.* 1991). A detailed description of the first and second-order texture variables that were used in this study are provided in Table 2. The present study uses and compares a wide range of first and second-order texture measures to assess forest damage caused by *S. noctilio* infestation.

Several window sizes may be used because smaller windows capture the textural characteristics of individual objects such as trees, while larger windows capture the textural characteristics of larger area such as forest stands (Moskal & Franklin 2001). However, this will vary according to image resolution. The most appropriate window size is often found through trial and error (Kayitakire *et al.* 2006). In this study, five first-order (occurrence) texture measures were calculated, namely: data range, entropy, mean, skewness, and variance. The analysis was performed using five different window sizes (3 × 3; 5 × 5; 7 × 7; 9 × 9 and 11 × 11 pixels). Eight second-order (co-occurrence) texture measures were then calculated (mean, variance, homogeneity, contrast, dissimilarity, entropy, second moment, correlation), using the same five window sizes. The texture variables were calculated in ENVI 4.3 (RSINC 2006). Once the 13 texture measures were calculated, the texture information was extracted for each sample plot (n = 65) using zonal statistics functionality in ArcGIS (ESRI 2006). Owing to the large number of mean texture variables (n = 260), the significant texture variables needed to be identified in order to simplify the modelling process.

Statistical analysis

All statistical tests were performed using Statistica 7.1 (StatSoft 2006). The Shapiro-Wilk test was used to test for normality, followed by a correlation analysis to test the relationship between texture measures and levels of *S. noctilio* infestation. The significant variables were then entered into a forward stepwise linear regression. Linear regression relates one variable to a single (simple regression) or combination (multiple regression) of variables. The multiple regression is a very popular method and is often used to predict the spatial distribution of phenomena (Guisan & Zimmermann 2000). For example, a stepwise linear regression equation was used to successfully assess hemlock decline caused by the forest pest, hemlock woolly adelgid, *Adelges tsugae* Annand, in North America (Pontius *et al.* 2005). Similarly, a regression model was used to determine the spatial distribution of beech-fir, *Albieti fagetum,* damage in Croatia (Bozic *et al.* 2006).

In this study the significant texture variables (n = 35) were entered into a forward stepwise multiple regression model to determine if *S. noctilio* infestation levels could be predicted using image texture. To avoid problems of over-fitting, the maximum number of steps in the forward stepwise regression was set at seven. This avoids unstable regression line predictions which are unlikely to recur if the experiment is repeated (Serrano *et al.* 2002).

RESULTS

Correlation tests were run to determine if there is a significant relationship between the calculated texture measures and *S. noctilio* infestations. The resulting correlation coefficients for both the first and second-order texture measures were average in strength. The highest correlation coefficient was 0.49 for the second-order correlation statistic in the NIR band using a 3 × 3 window size. Fig. 4 shows examples of scatterplots from the analysed data. The near infrared (NIR) band showed significant correlation with *S. noctilio* infestation. The blue band also resulted in a significant relationship with *S. noctilio* infestation, especially in

Table 2. Texture algorithms calculated from the high-resolution satellite image.

Type of measure	Measure	Formula	Description	Example: blue band (3 × 3 window)
First-order	Entropy	$\sum_{i=0}^{G-1} p(i)\log_2[p(i)]$ Where G is the total number of intensity levels	Entropy is a measure of histogram uniformity (Materka & Stralecki 1998)	
	Data range	$\max\{X\}-\min\{X\}$ Where $X = x_1, x_2, \ldots, x_k$	Measures the range of the pixel data (St-Louis *et al.* 2006)	
	Mean	$\text{AVG} = \frac{\sum_k x_k}{K}$	The mean calculates the average texture value at each plot (St-Louis *et al.* 2006)	
	Skewness	$\mu_3 = \sigma^{-3}\sum_{1=0}^{G-1}(i-\mu)^3 p(i)$ Where G is the total number of intensity levels	Measures the skewness of the data set, if the skewness is 0 the histogram is equal about the mean (Materka & Stralecki, 1998).	
	Variance	$\frac{\sum(x_{ij}-M)^2}{n-1}$ Where x_{ij} is the digital number of the pixel (i, j), and n is the number of pixels in the moving window (ERDAS, 1997).	The variance texture measure accounts for the variability of the spectral response of pixels (Trutter *et al.* 2006)	
Second-order	Contrast	$\sum_{i,j=0}^{N-1} P_{i,j}(i-j)^2$	Contrast is a measure of the overall amount of local variation in a window (i.e. it is proportional to the range of grey levels) (Yuan *et al.* 1991)	
	Dissimilarity	$\sum_{i,j=0}^{N-1} P_{i,j}\lvert i-j\rvert$	The dissimilarity measure is similar to the contrast measure. However, where contrast weights increase exponentially (0, 1, 4, 9, etc.) as one moves away from the diagonal, dissimilarity weights increase linearly (0, 1, 2, 3, etc.) (Hall-Beyer 2007).	

Continued on p. 00

the first-order entropy and data range, and the majority of the second-order measures. The green and red bands did show some correlation with *S. noctilio* but not to the same extent as the NIR and blue bands. Window sizes are very important in a texture analysis as they detect various levels of change in image texture.

The texture variables calculated with a 3 × 3, 5 × 5, 7 × 7 moving window showed significant results principally in the blue and NIR bands. The measures calculated with the 9 × 9 and 11 × 11 window sizes showed significant results in all the

Table 2 (*continued*)

Type of measure	Measure	Formula	Description	Example: blue band (3 × 3 window)
Second-order	Homogeneity	$\sum_{i,j=0}^{N-1} \frac{P_{i,j}}{1+(i-j)^2}$	Homogeneity measures the smoothness of image texture. Large changes in spectral values will result in very small homogeneity values, while small changes will result in larger homogeneity values (Tuttle *et al.* 2006).	
	Second moment	$\sum_{i,j=0}^{N-1} P_{i,j}{}^2$	Second moment or angular second moment is a measure of homogeneity. A small second moment value indicates contrast in image texture while a large second moment value shows that the image is quite homogeneous (Yuan *et al.* 1991).	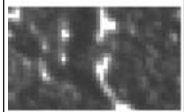
	Entropy	$\sum_{i,j=0}^{N-1} P_{i,j}\left(-\ln P_{i,j}\right)$	Entropy is a statistical measure of uncertainty. It is low if image texture is relatively smooth and high if the texture is structured. It can be used as a measure of the absence of a distinct structure or organization of image patterns (Yuan *et al.* 1991).	
	Mean	$\mu_i = \sum_{i,j=0}^{N-1} i\left(P_{i,j}\right)$ $\mu_j = \sum_{i,j=0}^{N-1} j\left(P_{i,j}\right)$	Average probability of grey-level co-occurrence (Lévesque & King 2003).	
	Variance	$\sigma_i^2 = \sum_{i,j=0}^{N-1} P_{i,j}\left(i-\mu_i\right)^2$ $\sigma_j^2 = \sum_{i,j=0}^{N-1} P_{i,j}\left(j-\mu_j\right)^2$	Accounts for the variability of the spectral response of pixels (Trutter *et al.* 2006) but considers the pairwise combinations of variability.	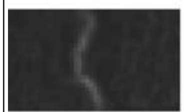
	Correlation	$\sum_{i,j=0}^{N-1} P_{i,j}\left[\frac{\left(i-\mu_i\right)\left(i-\mu_j\right)}{\sqrt{\left(\sigma_i^2\right)\left(\sigma_j^2\right)}}\right]$	The correlation texture algorithm measures the grey level linear-dependency within the image (Kayitakire *et al.* 2006)	

bands, with the highest correlations in the blue band. These results indicated that image texture is a significant indicator of *S. noctilio* infestation levels.

Regression analysis

The forward stepwise multiple regression analysis using the significant texture variables (n = 35) resulted in an R^2 value of 0.54 ($P \leq 0.01$).

Table 3 shows the bands, texture variables and window sizes of the significant variables used in the multiple regression equation.

The prediction accuracy of the model was calculated by plotting the observed *S. noctilio* infesta-

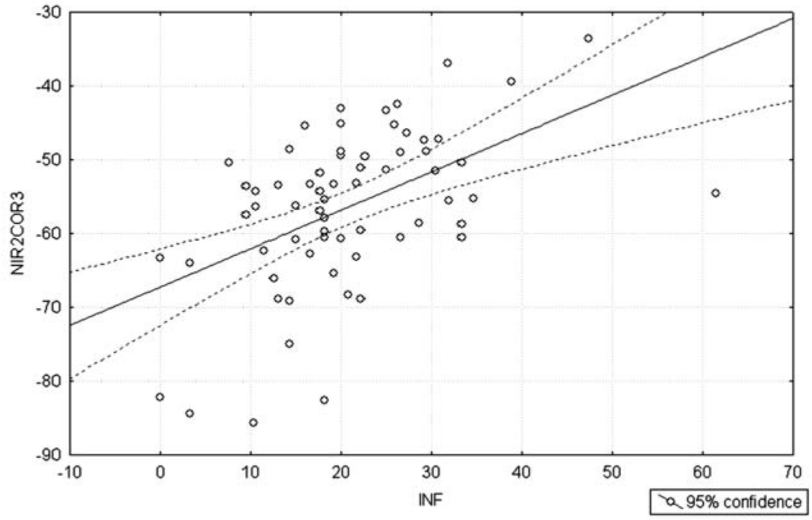

Second-order correlation (3 × 3):
$r = 0.49$

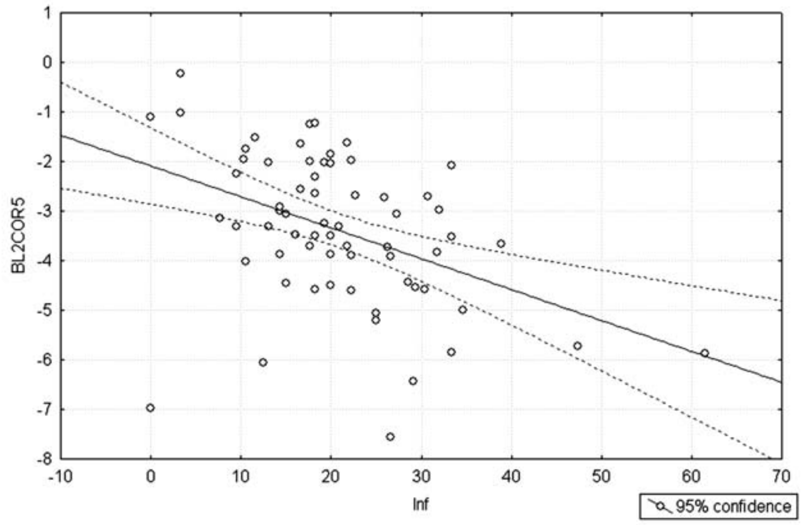

Second- order blue correlation (5 × 5):
$r = -0.43$

Fig. 4. Scatter plots showing significant correlations ($P < 0.05$) between texture measures and *Sirex noctilio* infestation levels. The texture variables are defined in Table 2. (*Continued on page 00*)

tion values against the predicted values from the equation. The result (Fig. 5) showed a strong correlation of $r = 0.74$ ($P < 0.01$), which indicated that the significant texture variables entered into a forward stepwise multiple regression could significantly predict the visible stages of *S. noctilio*-infestation.

The regression equation was then entered into ArcMap to create a prediction of *S. noctilio* infested trees for the entire study area and the results are presented in Fig. 6. The inserts (a) and (b) in Fig. 6 show the colour composite image and the predicted levels of infestation, respectively, following linear regression on the texture images. The

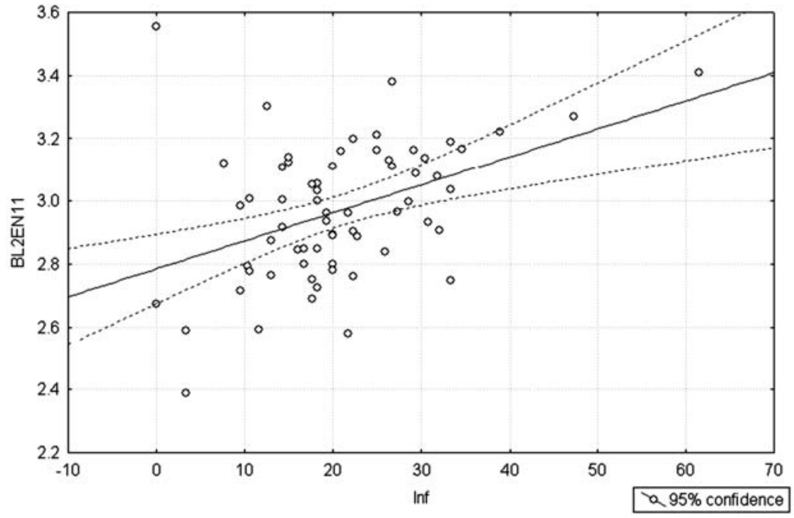

Second - order blue entropy (11 × 11):
$r = 0.43$

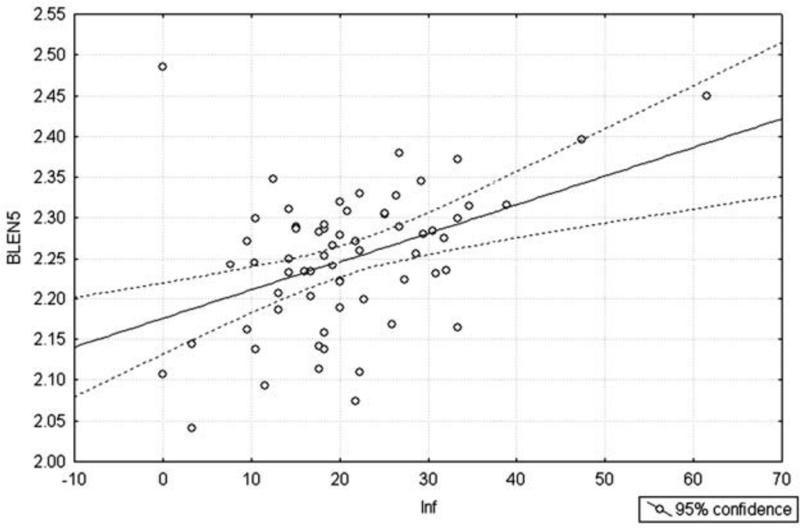

First order blue entropy (5 × 5):
$r = 0.43$

Fig. 4 (*continued*).

results on their own show how accurate texture measures are in predicting *S. noctilio* infestation as in insert (b).

DISCUSSION

Given the average correlations of individual texture measures to *S. noctilio* infestation, a stepwise multiple regression analysis was undertaken to determine whether a number of texture measures could have a stronger correlation with *S. noctilio* infestation. The multiple regression analysis resulted in an R^2 value of 0.55 ($P < 0.01$). A plot of the observed *S. noctilio* infestation levels against predicted values showed a correlation of 0.74 ($P < 0.01$), which meant that the regression equation

Table 3. Betas used in the forward stepwise multiple regression.

Band	1st or 2nd order	Texture variable	Window size	Abbreviation
Blue	2nd order	Correlation	5 × 5	BL2COR5
NIR	2nd order	Correlation	3 × 3	NIR2COR3
NIR	2nd order	Variance	11 × 11	NIR2VAR11
Blue	1st order	Variance	5 × 5	BLVAR5
NIR	2nd order	Variance	9 × 9	NIR2VAR9
Blue	1st order	Data Range	3 × 3	BLDR3
Blue	2nd order	Entropy	3 × 3	BL2EN3

could significantly predict the visible stages of *S. noctilio* infestation.

The results from the regression analysis indicated that the smaller window sizes (3 × 3 and 5 × 5) were significant predictors of *S. noctilio* infestation. This is perhaps due to the fact that smaller window sizes can detect subtle textural changes in individual tree crowns caused by defoliation. On the other hand, the 9 × 9 and 11 × 11 NIR variance texture variables were significant in the regression analysis. This shows that it is also necessary to consider textural changes over larger areas in order to detect variance within a stand. The results from this study indicate that it is more effective to use a variety of window sizes instead of simply using the smallest window size.

The 35 significant texture variables and the significant betas from the regression analysis were dominated by the blue and NIR bands. Leaf reflectance is determined by the concentrations of pigments such as chlorophyll and carotene. These leaf characteristics vary greatly, which in turn affects the leaf reflectance properties. Healthy plants will contain high levels of chlorophyll *a* and *b*, as well as carotene (Schmidt 2003). As tree health declines, the concentrations of pigments will decrease and this can be detected in the chlorophyll-sensitive blue band. This is why the blue band showed high correlation with *S. noctilio* infestation. The NIR band also showed strong correlation with *S. noctilio* infestation. This is because vegetation reflects highly in the NIR portion of the electromagnetic spectrum. Healthy trees will reflect more in the NIR, but as tree health

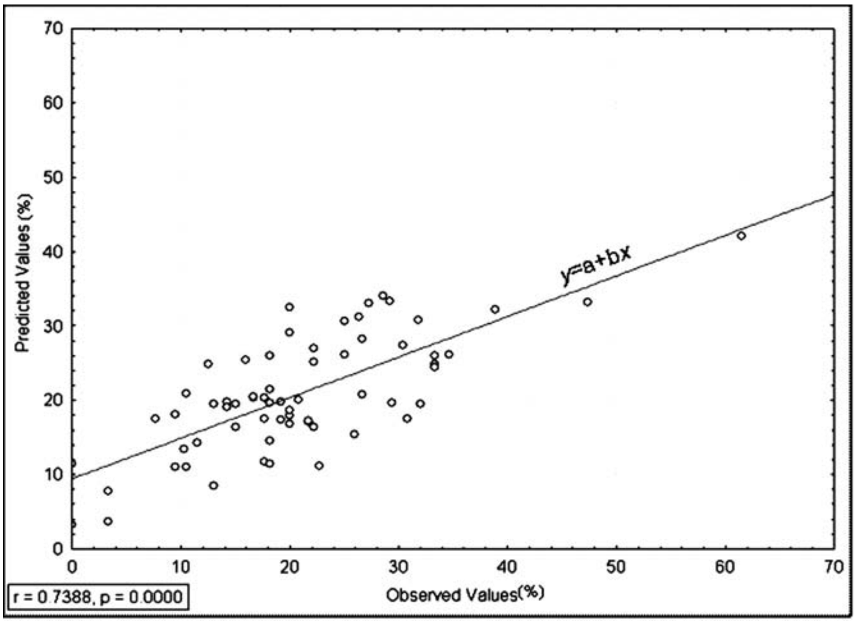

Fig. 5. Predicted *versus* observed values of *Sirex noctilio* infestation using a regression model.

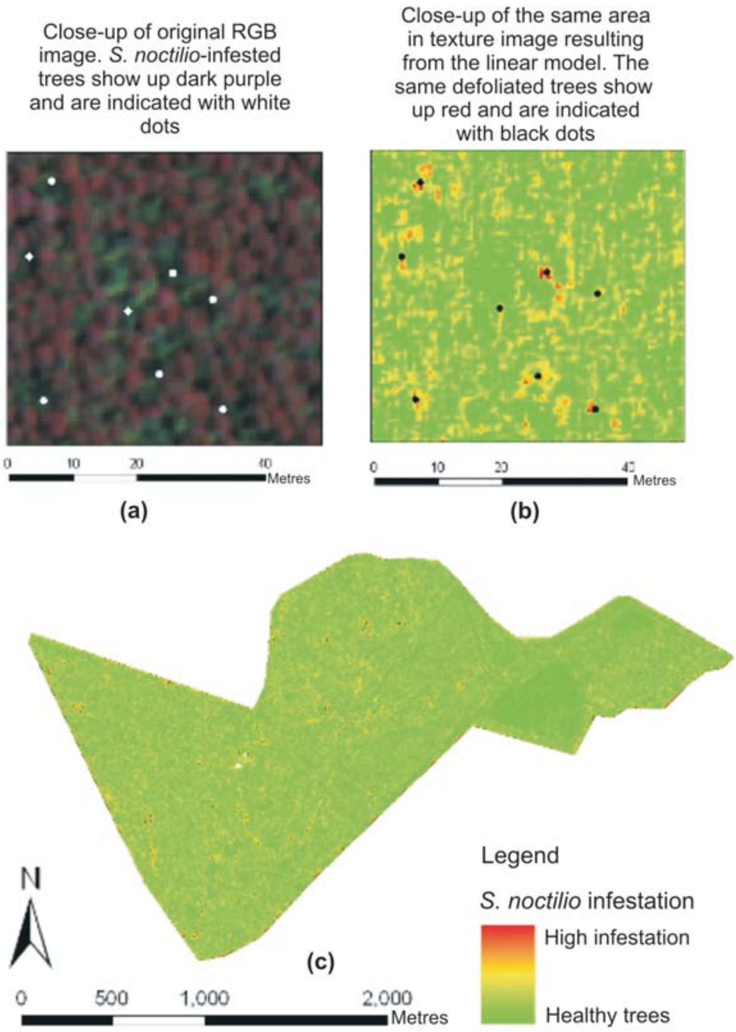

Fig. 6. Map showing the severity and extent of *Sirex noctilio* infestation.

declines, the NIR reflectance will decrease providing a good indication of insect infestation.

Three of the seven significant texture variables from the regression analysis were variance statistics which measure the variability of the spectral response of the pixel values (Tuttle *et al.* 2006). Variance is successful in detecting infested trees as it picks up the subtle changes in image texture due to tree health decline. The correlation and entropy texture variables that were selected indicate the importance of the linear dependency of pixel values within a window. This is useful in clumping together pixels that share the same characteristics for example pixels showing areas of defoliation.

In summary, the results from this study indicated that it is more effective to consider a number of texture variables which measure different levels of texture variation. Furthermore, our findings indicate that although it is generally accepted that second-order texture measures are a better texture representation method (Yuan *et al.* 1991), one must not overlook the value of first-order texture measures. Out of the 35 significant texture variables entered into the regression equation, 14 were first-order statistics.

In conclusion, this study has shown that first and second-order texture measures calculated from high-resolution spatial imagery can significantly predict the visual (red and grey) stages of *S. noctilio* infestation. By using a number of texture variables, more textural information is obtained as each texture measure has its strength and will detect subtle changes that another texture measure will not.

The results offer a useful tool to forest managers in assessing the spatial occurrence and severity of *S. noctilio* infestations in pine plantations. The successful implementation of biological and silvicultural methods in controlling *S. noctilio* populations strongly depends on such a tool in quantifying the severity and extent of infestation. However, we recommend that future studies look at the edge effects on the reflectance signals, an optimal spatial sampling scheme for the detection of *S. noctilio* infested trees, and an improvement in the methods used to identify infected trees.

ACKNOWLEDGEMENTS

We thank M. Norris Rogers from Mondi for providing the image data and the referees for valuable comments on the paper.

REFERENCES

ATKINSON, P.M., WEBSTER, R. & CURRAN, P.J. 1992. Cokriging with ground-based radiometry. *Remote Sensing of Environment* **41**: 45–60.

BOZIC, M., ANTONIC, O., PERNAR, P., JELASKA, S.D., CAVLOVIC, J. & KUSAN, V. 2006. Modelling the damage status of silver fir trees (*Albies alba* Mill.) on the basis of geomorphological, climatic and stand factors. *Ecological Modelling* **194**: 202–208.

CARLSON, J. & VERSCHOOR, K. 2006. *Insect Invasion.* New York State Conservationists. New York.

CARTER, G.A. & KNAPP, A.K. 2001. Leaf optical properties in higher plants: linking spectral characteristics to stress and chlorophyll concentration. *American Journal of Botany* **88**: 667–684.

ESRI 2006. *ArcGIS Version 9.1.* ERSI, California.

FORESTRY TASMANIA 1999. *Identifying pests in Tasmanian forests: Information sheet 7.* Forest Tasmania, City.

FRANKLIN, S.E., HALL, R.F.J., MOSKAL, L.M., MAUDIE, A.J. & LAVIGNE, M.B. 2000. Incorporating texture into classification of forest species composition from airborne multispectral images. *International Journal of Remote Sensing* **21**: 61–79.

FRANKLIN, S.E., WULDER, M.A, SKAKUN, R & CARROLL, A, 2003, Mountain pine beetle red attack damage classification using stratified Landsat TM data in British Columbia, Canada. *International Journal of Remote Sensing* **69**: 283–288.

GUISAN, A. & ZIMMERMANN, N.E. 2000. Predictive habitat distribution models in ecology. *Ecological Modelling* **135**: 147–186.

HALL-BEYER, M. 2007. *The GLCM Tutorial Home Page.* University of Calgary. Canada. Online at: http://www.ucalgary.ca (accessed Month year)

HAARA, A. & NEVALAINEN, S. 2002. Detection of dead or defoliated spruces using digital aerial data. *Forest Ecology and Management* **160**: 97–107.

HARRALICK, R.M., SHANMUGAM, K. & DINSTEIN, I. 1973. Textural features for image classification. *IEEE Transactions on Systems, Man, and Cybernetics, SMC* **3**: 610–621.

HOEBEKE, E.R., HAUGEN, D.A. & HAACK, R.A. 2005. *Sirex noctilio:* discovery of a Palearctic siricid woodwasp in New York. *Newsletter of the Michigan Entomological Society* **50**(1&2): 24–25.

ISMAIL, R., MUTANGA, O & BOB, U. 2007. Forest health and vitality: the detection and monitoring of *Pinus patula* trees infected by *Sirex noctilio* using digital ultispectral imagery (DMSI). *Southern Hemisphere Forestry Journal* **69**: 39–47.

ISMAIL, R., MUTANGA, O. & BOB, U. 2006. The use of high resolution airborne imagery for the detection of forest canopy damage by *Sirex noctilio.* In: Langin P.A. & Antonides M.C. (Eds) *Precision Forestry in Plantations, Semi-natural Areas and Natural Forests. Proceedings of the International Precision Forestry Symposium*, Stellenbosch University, Stellenbosch, South Africa.

JOBANPUTRA, D.A.C. 2006. Preserving boundaries for image texture segmentation using grey level co-occurring probabilities. *Pattern Recognition* **39**: 234–245.

KATSCH, C. & VOGT, H. 1999. Remote sensing from space – present and future applications in forestry, nature conservation and landscape management. *Southern African Forestry Journal* **185**: 14–25.

KAYITAKIRE, C., HAMEL, C. & DEFOURNY, P. 2006. Retrieving forest structure variables based on image texture analysis and IKONOS-2 imagery. *Remote Sensing of Environment* **102**: 390–401.

KING, D.J. 2000. Airborne remote sensing in forestry: sensors, analysis and applications. *The Forestry Chronicle* **76**: 25–42.

LÈVESQUE, J. & KING, D.J. 2003. Spatial analysis of radiometric fractions from high-resolution multispectral imagery for modelling individual tree crown and forest canopy structure and health. *Remote Sensing of Environment* **84**: 589–602.

MATERKA, A. & STRALECKI, M. 1998. *Texture analysis methods – A review.* Technical University of Lodz. Brussels.

MOSKAL, L.M. & FRANKLIN, S.E. 2001. Classifying multilayer forest structure and composition using high resolution, compact airborne spectrographic imager image texture. *American Society of Remote Sensing and Photogrammetry Annual Conference,* day/s Month year, St-Louis, State.

MOSKAL, L.M. & FRANKLIN, S.E. 2004. Relationship between airborne multispectral image texture and aspen defoliation. *International Journal of Remote Sensing* **25**: 2701–2711.

MUTANGA, O. & RUGEGE, D. 2006. Integrating remote sensing and spatial statistics to model herbaceous biomass distribution in a tropical savanna. *Interna-*

tional Journal of Remote Sensing **27**(16): 3499–3514.

MYINT, S.W. & LAM, N. 2005. A study of lacunarity-based texture analysis approaches to improve urban image classification. *Computers, Environment and Urban Systems* **29**: 501–523.

PONTIUS, J., HALLETT, R. & MARTIN, M. 2005. Using AVIRIS to assess hemlock abundance and early decline in the Catskills, New York. *Remote Sensing of Environment* **97**: 163–173.

RSINC 2006. *ENVI Version 4.3.* ITT Industries. Colorado.

SCHMIDT, K.S. 2003. *Hyperspectral remote sensing of vegetation species distribution in Saltmarsh.* International Institute for Geo-Information Science and Earth Observation, City, the Netherlands.

SCHULZE, R.E., MAHARAJ, M., LYNCH, S.D., HOWE, B.J. & MELVIL-THOMSON, B. 1997. *South African Atlas of Agrohydrology and Climatology.* Water Research Commission Report TT82/96.

SERRANO, L., PENUELAS, J. & USTIN, S. 2002. Remote sensing of nitrogen and lignin in Mediterranean vegetation from AVIRIS data: decomposing biochemical from structural signals. *Remote Sensing of Environment* **81**: 355–364.

SLIPPERS, B., WINGFIELD, M.J., COUTINHO, T.A. & WINGFIELD, B.D. 2003. A review of the genus *Amylostereum* and its associated woodwasps. *South African Journal of Science* **99**: 70–74.

STATSOFT 2006. *Statistica Version 7.1.* Statsoft Inc. City, Oklahoma.

ST-LOUIS, V., PIDGEON, A.M., RADELOFF, V.C., HAWBAKER, T.J. & CLAYTON, M.K. 2006. High-resolution image texture as a predictor of bird species richness. *Remote Sensing of Environment* **105**: 299–312.

TRIBE, G. 2006. A wasp counterattack to save pine trees. *Village Life* **18**: 38–40.

TRIBE, G.D. & CILLIE, J.J. 2004. The spread of *Sirex noctilio* Fabricius (Hymenoptera: Siricidae) in South African pine plantations and the introduction and establishment of its biological agents. *African Entomology* **12**: 9–17.

TUTTLE, E.M., JENSON, R.R., FORMICA, V.A. & GONSER, R.A. 2006. Using remote sensing image texture to study habitat use patterns: a case using the polymorphic white-throated sparrow (Zono) (*Zonptrichia albocollis*). *Global Ecology and Biogeography* **15**: 349–357.

USDA 2000. *Forest Health Update: Enterprise Team Update.* United States Department of Agriculture, City, Colorado.

YUAN, X., KING, D. & VLECK, J. 1991. Sugar maple leaf decline assessment based on spectral and textural analysis of multispectral aerial videography. *Remote Sensing of Environment* **37**: 47–54.

ZONDAG, R. & NUTTALL, M.J. 1999. Sirex *woodwasp: Forest and Timber Insects in New Zealand.* Forest Research Institute, Rotorua.

Accepted 3 July 2008